Ion-source and LEBT Issues with the Front-End Systems for the Spallation Neutron Source*

R. Keller, D. Cheng, R. DiGennaro, R.A. Gough, J. Greer, K.N. Leung, A. Ratti, J. Reijonen, R.W. Thomae, T. Schenkel, J.W. Staples, and R. Yourd, *E. O. Lawrence Berkeley National Laboratory, Berkeley, CA, USA*

A. Aleksandrov, M.P. Stockli, and R.W. Welton, *Oak Ridge National Laboratory, Oak Ridge, TN, USA*

Abstract: The Front-End Systems (FES) of the Spallation Neutron Source (SNS) project are being built by Berkeley Lab and will deliver a pulsed 40-mA H^- ion beam at 2.5 MeV energy to the subsequent Drift-Tube Linac. The FES accelerator components comprise an rf driven, volume-production, cesium-enhanced, multi-cusp Ion Source; an electrostatic Low-Energy Beam Transport (LEBT) that includes provisions for transverse focusing, steering, and beam chopping; an RFQ accelerator; and a Medium-Energy Beam Transport (MEBT) line. The challenges for Ion Source and LEBT design are the generation of a plasma suitable for creating the required high H^- ion density, lifetime of the rf antenna at 6% duty factor, removal of the parasitic electron population from the extracted negative ions, and emittance conservation. The paper discusses these issues in detail and highlights key experimental results obtained so far.

*This work is supported by the Director, Office of Science, Office of Basic Energy Sciences, of the U.S. Department of Energy under Contract No. DE-AC03-76SF00098.

1. Introduction

Berkeley Lab is presently building the Front-End Systems (FES), a 2.5-MeV linac injector for the Spallation Neutron Source (SNS) project under construction at Oak Ridge National Laboratory. The main FES subsystems consist of Ion Source, Low-Energy Beam-Transport (LEBT) section, Radio-Frequency Quadrupole (RFQ) accelerator, and Medium-Energy Beam-Transport (MEBT) section. The SNS Front-End project has been described in detail elsewhere with an ample collection of references [1], and an updated progress report has been given recently [2]. A 3-dimensional CAD layout of the front-end beamline is shown in Figure 1.

The SNS accelerator systems aim at delivering intense proton-beam pulses of less than 1-μs duration to the spallation target at 60-Hz repetition frequency and with an average beam power of 1.44 MW. The 1-ms long H^- macro pulses that are accelerated in the linac to 1-GeV energy must be chopped into 'mini pulses' of 645-ns duration, with 300-ns long gaps. Chopping is performed in the Front End by two separate chopper systems located in LEBT and MEBT, respectively. The LEBT chopper removes most of the beam power during the mini-pulse gaps, and the MEBT chopper reduces the rise and fall time of the transported beam and cleans out the beam current still present in the gaps. The key performance parameters for the SNS Front-End Systems are listed in Table 1.

The major challenges for Ion Source and LEBT design are the generation of a plasma suitable for creating the required high H^- ion density, lifetime of the rf antenna at 6% duty factor,

removal of the parasitic electron population from the extracted negative ions, formation of a low-emittance ion beam, and emittance conservation. This paper discusses these issues in detail and highlights key experimental results obtained so far with Ion Source, LEBT, and the first of four RFQ modules.

Table 1. FES Key Performance Parameters

Ion species	H^-
Output energy (MeV)	2.5
H^- peak current:	
MEBT output (mA)	38
Nominal ion-source output (mA)	50
Output normalized transverse rms emittance (π mm mrad)	0.27
Output normalized longitudinal rms emittance (π MeV deg)	0.126
Macro pulse length (ms)	1
Duty factor (%)	6
Repetition rate (Hertz)	60
Chopper system:	
LEBT rise, fall time (ns)	50
MEBT rise, fall time (ns)	10
Off/on beam-current ratio	10^{-4}

2. Ion Source Design

The H^- Ion Source and LEBT are shown in Fig. 2. The source plasma is sustained by pulsed 2-MHz rf power that is conducted to an internal rf antenna through a transformer-based impedance-matching unit and confined by a multi-cusp magnet field created by a total of 20 samarium-cobalt magnets lining the cylindrical chamber wall and 4 magnets lining the back

plate. A magnetic dipole filter separates the main plasma from a smaller H^- production region (darker area in Fig. 2) where low-energy electrons facilitate the generation of copious amounts of negative ions. A heated collar, equipped with eight cesium dispensers, surrounds this H^- production volume. The rf antenna is made from copper tubing, coiled to 2 1/2 windings, and water cooled. A 0.2-mm thick porcelain layer insulates the plasma from the oscillating antenna potentials. The actual composition and thickness of this coating layer is of utmost importance for the lifetime and reliability of the ion source and is discussed in detail elsewhere [3].

The outlet plate of the ion source contains another magnet system in Halbach configuration [4] that creates a dipole field across the extraction gap in order to separate extracted electrons from the ion beam and steer them towards a ‘dumping’ electrode biased at about 5 kV with respect to the outlet plate. Because this dumping field steers the ion beam as well, the entire plasma generator is tilted at an adjustable angle of about 3° against the LEBT axis to compensate for this effect.

Ignition of the discharge at the beginning of every macro pulse and at the optimum gas pressure for copious H^- production is rather difficult, and after trying out various scenarios including a heated filament and UV light bursts generated either by a laser or by flash lamps, the method of choice consists of maintaining a continuous-wave (cw) rf discharge sustained by about 100 W of 13.56-MHz rf power that is fed to the antenna through a separate, capacitive matching unit [5]. In the presence of the steady-state low-density plasma sustained by this

second rf system, the ramping time of the main discharge pulse is accelerated by about 25 μs as compared to using the 2-MHz rf alone.

Cesiation of the source surfaces adjacent to the outlet aperture is an essential aspect of creating intense H^- ion beams for two reasons [6]. On one hand, a minute amount of cesium, about 1/2 a mono layer thick, can enhance the beam intensity by a factor of three. Secondly, the density of electrons that are extracted together with the negative ions is typically reduced by one order of magnitude, significantly easing the space-charge load that acts on the ion beam where the plasma meniscus is being formed. The strategy how to obtain the necessary cesium coverage was developed with the SSC ion source [7], the direct predecessor of the SNS source. Cesium is contained in eight small “getter wire” boxes that are inserted inside the cesium collar and open up at elevated temperature to release the cesium. A temperature in excess of 500°C is needed for this process to happen. Once the surfaces are well covered the temperature can be reduced to about 250°C for optimum H^- production rates. The amount of released cesium is so small that the cesium supply will last for months of full duty-factor operation, and an ion source that has been vented to atmosphere pressure after operation does not even have to be cleaned before pumping down again.

As discussed above, separation of parasitic electrons from the ion beam is provided by a magnetic dipole field generated by permanent magnets inside the outlet electrode. By assembling permanent magnets in two different layers with vertical and longitudinal field directions,

respectively, the field is directed away from the outlet plane and sharply peaks a few mm downstream of it with about 1600-G maximum flux density. In principle, the electrons are separated from the ions at very low energy and either reflected back onto the outlet electrode or deflected into the space between the outlet electrode and an additional ‘dumping’ electrode inserted in the main extraction gap.

The problem with this arrangement is that its functioning depends on the detailed magnetic field profile, on the general electrical field distribution in presence of an inhomogeneous space-charge cloud, and in particular on the location and shape of the plasma meniscus that separates the source plasma from the accelerated beam. During the ion-source development phase, the electrical field was simulated by using the code IGUN [8], but while its predictions of beam-transport properties in the LEBT section appear to be quite accurate, the beam-formation problem cannot be well modeled by such an positive-ion code. A recent, preliminary study [9] using the code PBGUNS [10] with its negative-ion option, points to a large discrepancy with respect to the meniscus location illustrated in Figure 3. If the meniscus, as indicated by the PBGUNS results, is indeed located several mm farther downstream of the outlet plane and much more curved as well, the ion beam would expand stronger than assumed on the base of IGUN simulations and would be more affected by spherical aberration in the extraction and lens areas, leading to heavier distorted emittance shapes and more pronounced beam halo. This effect is much more pronounced for the higher beam currents that SNS is ultimately aiming at.

Preliminary emittance measurements seem to confirm this general assessment, as will be discussed below, but a solution to this part of the problem was identified in the same simulation study [9], basically consisting in a modification to the outlet aperture contour with a very shallow angle instead of the steep, Pierce-inspired angle used in the standard design [11]. A still unresolved issue is the action of the dumping magnetic field in a situation where the meniscus is positioned very close to the peak field, as expected to happen with higher plasma density values. If too many electrons are directed back towards the source plasma the resulting space-charge cloud would adversely affect the quality of the extracted ion beam. This topic will have to be addressed once sufficient confidence in the PBGUNS results has been established.

3. LEBT Design

The current LEBT-electrode design as shown in Figure 2 evolved from earlier incarnations when at a certain phase in the SNS project the nominal LEBT beam-current requirement had been raised from 35 to 70 mA [12]. Even after the requirement was subsequently reduced to 50 mA as listed in Table 1, the new design appears to be better suited to reduce emittance distortions, with the caveat that it is based on positive-ion simulations using IGUN.

The LEBT electrodes consist mainly of the extractor and two electrostatic einzel lenses that provide two-parameter matching into the RFQ entrance plane. The central electrode of the second lens is split into four isolated quadrants, and electrostatic voltages can be superimposed

on the main lens potential to provide angular steering in the horizontal and vertical directions. In addition, the entire ion-source and LEBT structure can be mechanically shifted in both transverse directions with respect to the last LEBT electrode which also acts as the RFQ entrance flange. This shift would primarily result in another angular steering effect, but the actions of electrical and mechanical steering functions combine to provide lateral axis offsets as well.

Apart from this static steering function, the second lens center-electrode is also used to create the mini-pulse structure in the ion beam by superimposing fast voltage pulses on the static potentials. During the mini-pulse gaps, the beam will be deflected partially into the RFQ entrance flange and partially into the RFQ walls. By periodically alternating the voltages between opposing pairs of the lens quadrants, the deflected beam is rotated among four diagonal directions that line up with the empty spaces between the RFQ vanes, at 45° angles with respect to the horizontal and vertical planes. The RFQ entrance flange is equipped with four isolated quadrants on its upstream side to allow measuring current-asymmetries in the four directions and adjust the static steering voltages.

Mechanically, the entire source/LEBT assembly is supported on one large flange inside the LEBT tank as shown in Figure 4, providing high effective pumping speed in order to keep the background pressure as low as possible. With three 1000-l/s turbomolecular pumps this pressure typically amounts to 5×10^{-5} mbar under nominal conditions.

4. Beam Results

Most measurements on the Ion-Source/LEBT system were taken with a diagnostic chamber attached to the LEBT tank and a 13-mm diameter aperture in the LEBT end electrode, as opposed to the 7.5-mm aperture of the RFQ entrance wall. The diagnostic chamber contains a biased and magnetically shielded Faraday cup and two Allison-type electrostatic emittance scanners [13] for the horizontal and vertical directions. The experimental results obtained with this instrumentation are discussed elsewhere in more detail [14]. In addition, a first series of beam measurements has been performed with the first of four RFQ modules attached to the LEBT in place of the diagnostic chamber. For all results discussed here the beam energy was 65 keV, and the discharge duty factor varied between 0.1 and 6% with repetition rates between 10 and 60 Hz. Occasionally the duty factor was raised up to about 10% to speed up the cesium-collar heating process.

The H^- current output of the Ion Source, equipped with a 7-mm diameter outlet aperture, is proportional to the main 2-MHz rf power amplitude with a scaling factor of roughly 1 mA for 1 kW. The maximum beam current obtained so far is 50 mA pulse average, with a short peak value of 67 mA shortly after ignition of each pulse, as shown in Figure 5. A full matrix of LEBT focusing parameters was mapped to confirm that the RFQ matching conditions can be met [14]. With best matching of a 50-mA beam, the normalized 1-rms horizontal and vertical emittance

sizes were 0.33 π mm mrad and 0.30 π mm mrad, respectively. Figure 6 shows these emittance patterns, exhibiting significant distortions in their tails below the 10% intensity level.

The sputtering-limited antenna lifetime could not yet be truly assessed. The longest observed operation time at 6% duty factor amounted to 16 hrs and was determined by excessive build-up of metal coating on the antenna whose origin is still being investigated. It is expected that under regular operation conditions the antenna will function for several hundred hours.

The beam experiments with the first, 900-mm long, RFQ module were very successful as maximum beam transmission was reached on the first day of testing. For these tests, the extraction gap had been enlarged by 4.6 mm to ensure proper matching at the 30-mA current level aimed at for these initial tests. The 0-to-90% mini-pulse rise and fall times turned out to be 25-ns long, twice as fast as the previously measured high-voltage switching speed of 50 ns because the RFQ entrance-flange and cavity intercept essentially all of the chopped beam at less than the nominal chopping amplitude of ±2.5 kV.

The beam-transmission curve displayed in Figure 7 demonstrates how closely the actual behavior of the first RFQ module mirrors the predictions based on PARMTEQ simulations.

5. References

[1] R. Keller for the FES Team, "Status of the SNS Front-End Systems, Proceedings of **EPAC 2000,** Paper MOP5B04, Wien (2000).

[2] R. Keller et al., "Progress with the SNS Front-End Systems," Proceedings of **PAC 2001**, Paper MOPB005**,** Chicago (2001).

[3] R. F. Welton and M. P. Stockli, M. Janney, R. Keller, T. Schenkel, and R. Thomae, "Advanced material coatings of radio-frequency ion source antennas," these proceedings, **ICIS '01** Oakland (2001).

[4] K. Halbach, Nucl. Instrum. Methods 169, p.1 (1980).

[5] T. Schenkel, J.W. Staples, R.W. Thomae, J. Reijonen, R.A. Gough, K.N. Leung, R. Keller, R.F. Welton and M.P. Stockli, "Plasma Ignition Schemes for the SNS Radio-Frequency Driven H^- Source," these proceedings, **ICIS '01** Oakland (2001).

[6] K. N. Leung, D.A. Bachman, and D.S. McDonald, Rev. Sci. Instr. **64**, p. 970 (1993).

[7] K. Saadatmand, G. Arbique, J. Hebert, R. Valicenti, and K.N. Leung, "Performance of a High Current H^- Radio Frequency Volume Ion Source," Rev. Sci. Instr. **67 (3)**, p. 1318 (1996).

[8] R. Becker, "New Features in the Simulation of Ion Extraction with IGUN," Proceedings of **EPAC '98**, Stockholm (1998).

[9] R. F. Welton, M.P. Stockli, J.E. Boers, R. Runyair, R. Keller, J.W. Staples, and R.W. Thomae, "Simulation of the Ion Source Extraction and Low-Energy Beam Transport Systems for the Spallation Neutron Source Accelerator," these proceedings, **ICIS '01** Oakland (2001).

[10] J.E. Boers, PBGUNS Manual, available through Thunderbird Simulations, Garland, TX, 75042.

[11] M.A. Leitner, D.C. Wutte, and K.N. Leung, "2D Simulation and Optimization of the Volume H^- Ion Source Extraction system for the Spallation Neutron Source Accelerator," Nucl. Instrum. and Meth. **A 427**, 243 (1999).

[12] J. Reijonen, R. Thomae, and R. Keller, "Evolution of the LEBT Layout for SNS," Proceedings of **Linac 2000**, Monterey (2000).

[13] P.W. Allison, J.D. Sherman, and D.B. Holtkamp, IEEE Trans. Nucl. Sci, **NS-30**, p. 2204 (1983).

[14] R.W. Thomae, R.A. Gough, R. Keller, and K.N. Leung, "Measurements on the H^- Source and Low Energy Beam Transport System for the Spallation Neutron Source," these proceedings, **ICIS '01** Oakland (2001).

6. Figures and Captions

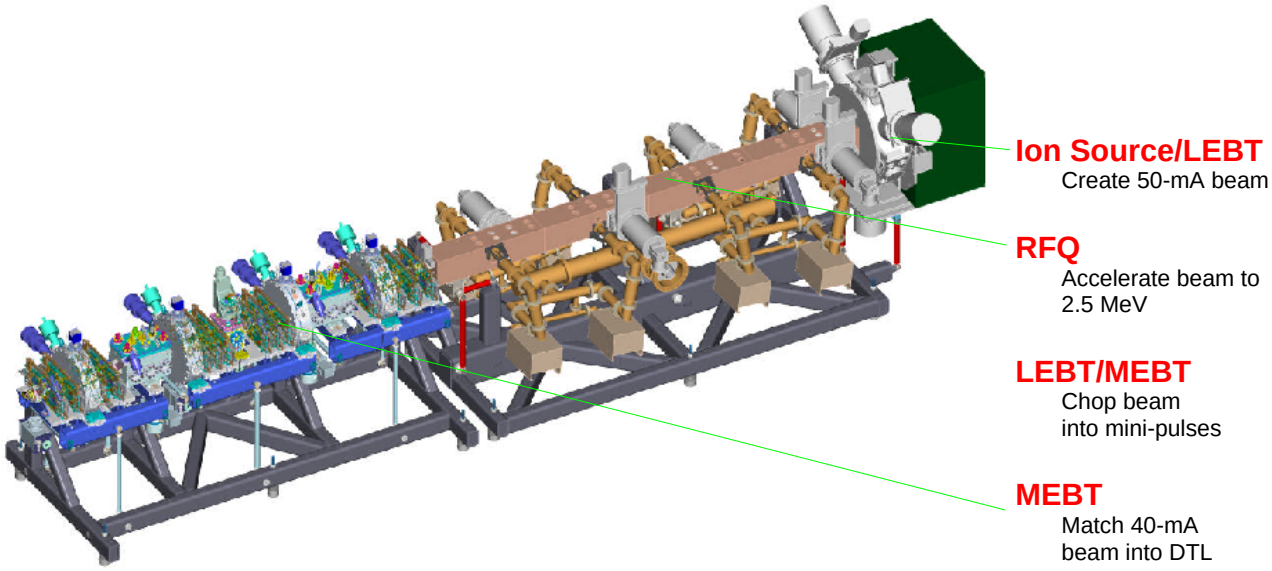

Figure 1. Layout of the SNS front-end beamline.

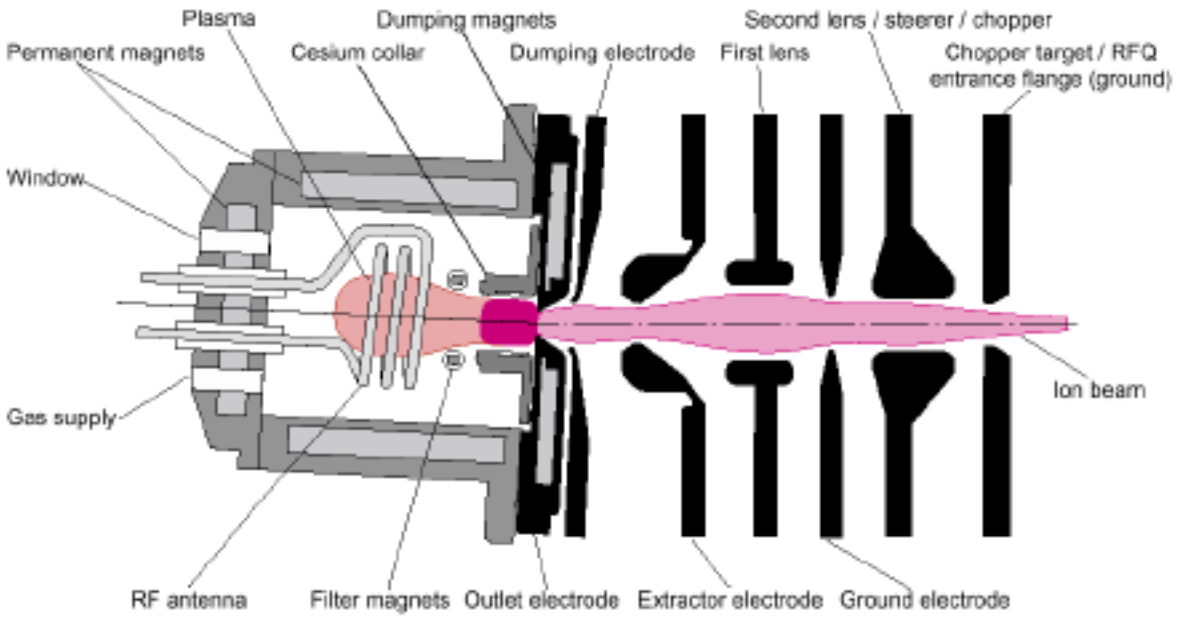

Figure 2. Schematic of the ion source and LEBT. Note that the actual filter and electron-dumping magnetic fields are oriented in anti-parallel directions, orthogonally to the illustration plane. The width of the ion beam is exaggerated in this schematic to emphasize the focusing action of the double-lens system.

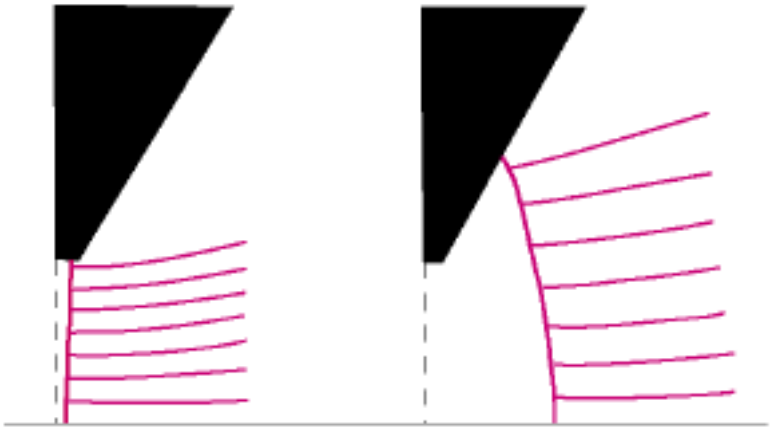

Figure 3. Comparison of plasma-meniscus locations with respect to the outlet aperture contours (black triangles) as resulting from simulations of the standard SNS ion-source extraction system [11], using the codes IGUN (left) and PBGUNS (right). Schematic ion-beam trajectories originating from these menisci are added, indicating significant differences in these simulation results.

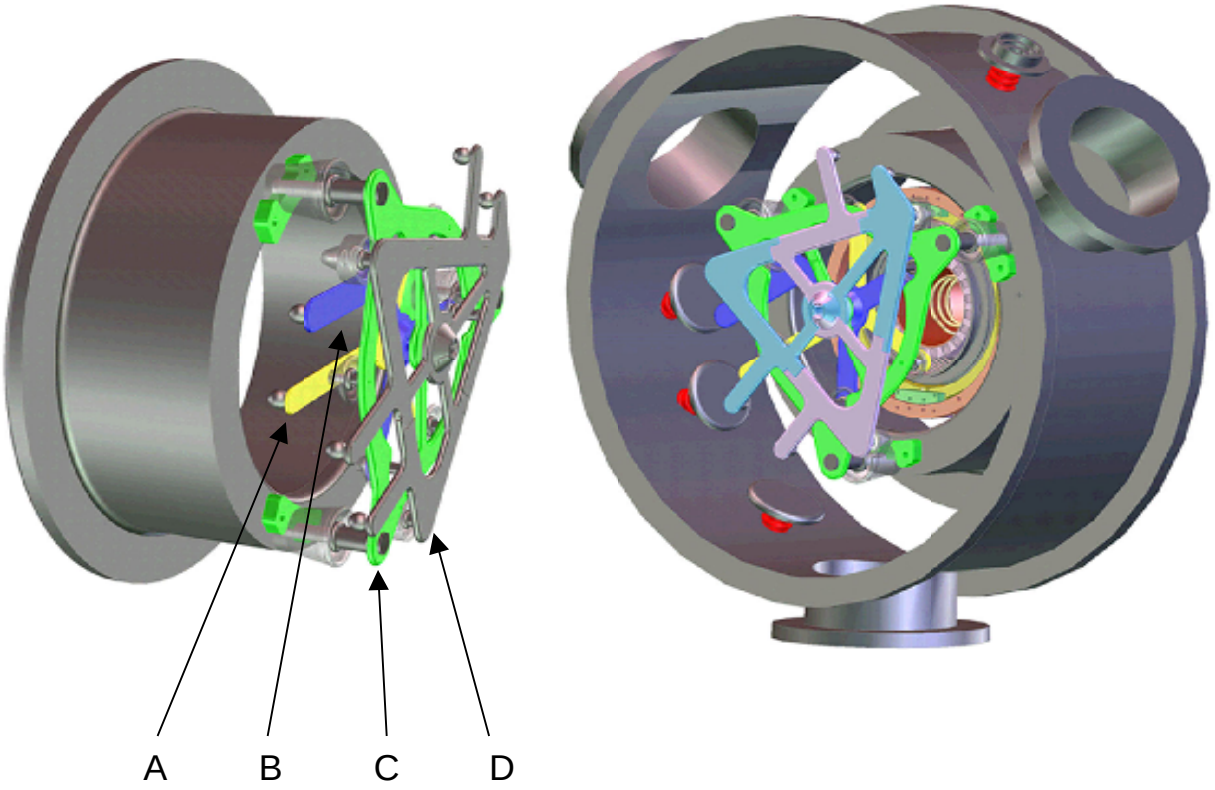

Figure 4. View of LEBT electrodes and their supports from the downstream side. Left, assembly on re-entrant flange; right, assembly inside LEBT vacuum tank with pumping ports. A, extractor; B, first lens; C, ground electrode; D, segmented second lens/steerer/chopper.

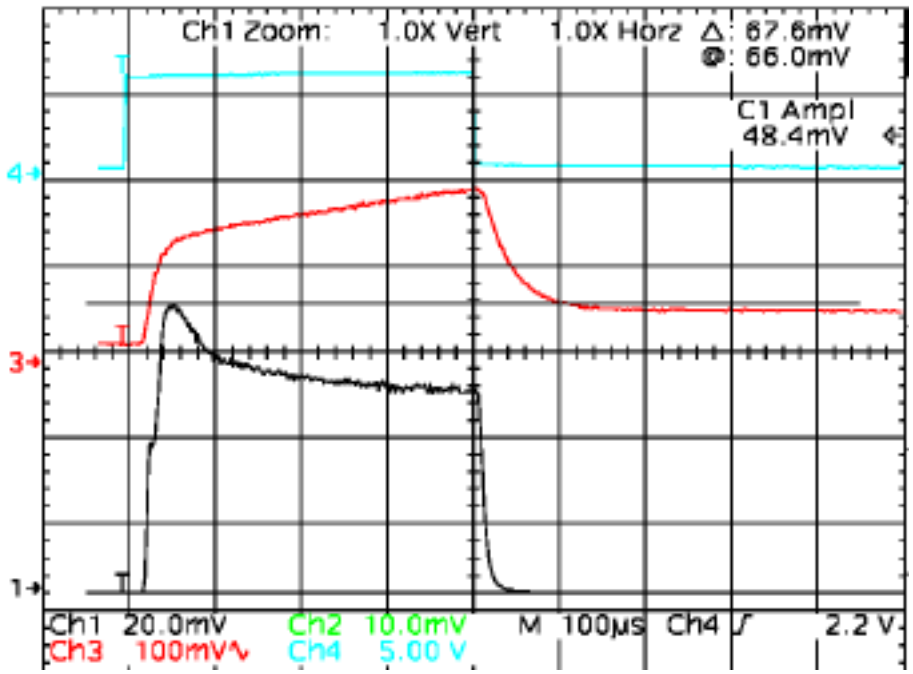

Figure 5. Maximum measured beam-current (black trace, channel 1): 68-mA peak and 50-mA average pulse height.

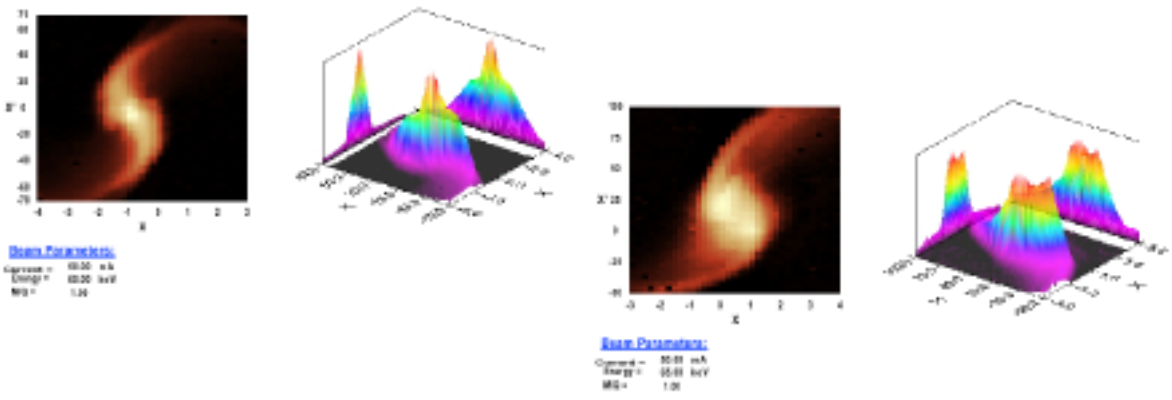

Vertical
0.3 π mm mrad

Horizontal
0.33 π mm mrad

Figure 6. Transverse emittances of a 50-mA beam, taken at the LEBT exit.

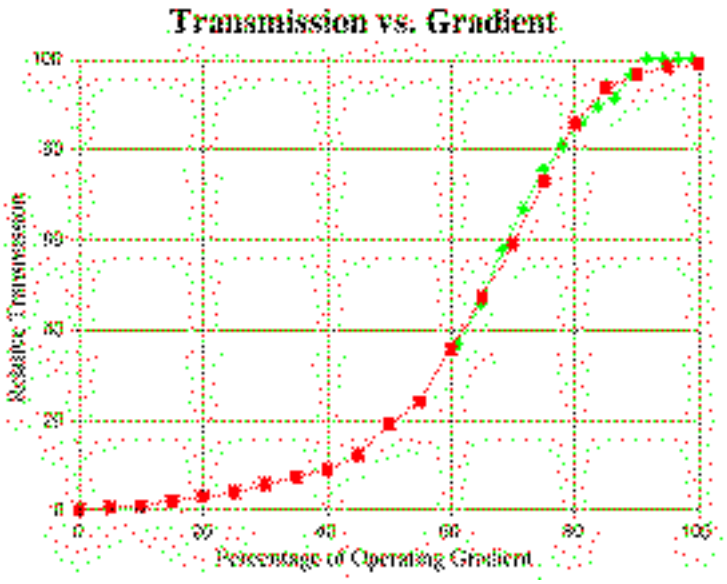

Figure 7. Simulated (red squares) and measured (green crosses) transmission curves of RFQ Module #1, normalized to 100% maximum, for an input beam of 35-mA.